

Effects of the nuclear equation of state on the r-mode instability and evolution of neutron stars

Ch.C. Moustakidis^{1,2}

¹Department of Theoretical Physics, Aristotle University of Thessaloniki,
54124 Thessaloniki, Greece and

²Theoretical Astrophysics, University of Tuebingen IAAT,
Auf der Morgenstelle 10, Tuebingen 72076 Germany

November 23, 2018

Abstract

I study the effect of nuclear equation of state on the r-mode instability of a rotating neutron star. I consider the case where the crust of the neutron star is perfectly rigid and I employ the related theory introduced by Lindblom *et al.* [1]. The gravitational and the viscous time scales, the critical angular velocity and the critical temperature are evaluated by employing a phenomenological nuclear model for the neutron star matter. The predicted equations of state for the β -stable nuclear matter are parameterized by varying the slope L of the symmetry energy at saturation density on the interval $72.5 \text{ MeV} \leq L \leq 110 \text{ MeV}$. The effects of the density dependence of the nuclear symmetry energy on r-mode instability properties and the time evolution of the angular velocity are presented and analyzed. A comparison of theoretical predictions with observed neutron stars in low-mass x-ray binaries (LMXBs) and millisecond radio pulsars (MSRPs) is also performed and analyzed. I estimate that it may be possible to impose constraints on the nuclear equation of state, by a suitable treatment of observations and theoretical predictions of the rotational frequency and spindown rate evolution of known neutron stars.

PACS number(s): 26.60.-c, 21.65.Ef, 04.40.Dg, 04.30.-w.

Keywords: Neutron stars; Nuclear equation of state; Nuclear symmetry energy; R-mode instability; Gravitational waves.

1 Introduction

The oscillations and instabilities of relativistic stars [2, 3, 4] gained a lot of interest in the last decades because of the possible detection of their gravitational waves [5, 6, 7, 8, 9, 10, 11, 12, 13, 14]. Especially neutron stars may suffer a number of instabilities which come in different flavors but they have a general feature in common, they can be directly associated with unstable modes of oscillation. In the present work I concentrate my study on the so called r-mode instability. The r-modes are oscillations of rotating stars whose restoring force is the Coriolis force. The gravitational radiation-driven instability of these modes has been proposed as an explanation for the observed relatively low spin frequencies of young neutron stars and of accreting neutron stars in low-mass X-ray binaries as well [1]. This instability can only occur when the gravitational-radiation driving time scale of the r-mode is shorter than the time scales of the various dissipation mechanisms that may occur in the interior of the neutron star.

A very interesting problem is the consideration of the effect on r-mode instability due to the presence of a solid crust in an old neutron star. It is proved that the presence of a viscous boundary layer under the solid crust of a neutron star increases the viscous damping rate of the fluid r-modes [1, 15]. Actually, the presence of a solid crust has a crucial effect on the r-mode motion and following the discussion of Andersson and Kokkotas [8] this effect can be understood as follows: based on the perfect fluid mode-calculations it is anticipated the transverse motion associated with the mode at the crust-core boundary to be large. However, if the crust is assumed to be rigid, the fluid motion must essentially fall off to zero at the base of the crust in order to satisfy a non-slip condition (in the rotating frame of reference).

Firstly, Bildsten and Ushomirsky [15], found that the shear dissipation in the viscous boundary layer between the solid crust and the fluid core decreases dramatically the viscous damping time in cold old neutron stars as well as in hot young neutron stars. They concluded that the r-mode instability is unlikely to play a role in old, accreting neutron stars where in hot young neutron stars the boundary-layer damping mechanism limits the ability of the

r-mode instability to reduce the angular momentum of the star and consequently to produce detectable amounts of gravitational radiation.

Anderson *et al.* [16] used various neutron-star parameters to obtain significantly different results for the critical frequency of the onset of r-mode instability. They found the critical velocity to be about 40% lower than the estimate of Bildsten and Ushomirsky and inferred that the r-mode instability is likely to be the mechanism that limits the LMXBs spin periods and those of other millisecond pulsars as well [16].

Rieutord [17] improved the model of the boundary layer and found that the critical velocity agrees rather closely with the original estimates of Bildsten and Ushomirsky. Lindblom [1] improved previous estimates of the damping rate by including the effect of the Coriolis force on the boundary-layer eigenfunction, using more realistic neutron-star models. They concluded that if the crust is assumed to be perfectly rigid, the gravitational radiation driven instability in the r-modes is completely suppressed in neutron stars colder than about 1.5×10^8 K and also found that the r-mode instability is responsible for limiting the spin periods of the LMXBs.

Wen *et al.* [18] studied the sensitivity of the neutron star r-mode instability window to the density dependence of the nuclear symmetry energy. Employing a simple model of a neutron star with a perfectly rigid crust constructed with a set of crust and core equations of state that span the range of nuclear experimental uncertainty in the symmetry energy, they concluded that smaller values of the slope parameter L of the symmetry energy help stabilize neutron stars against runaway r-mode oscillations. Vidana [19] analyzed also the role of the symmetry energy slope parameter L on the r-mode instability by using both microscopic and phenomenological approaches of the nuclear equation of state. He showed that the r-mode instability region is smaller for those models which give larger values of L . Alford *et al.* [20] studied the viscous damping of r-modes of compact stars and analyzed the regions where small amplitude modes are unstable to the emission of gravitational radiation. They showed that many aspects, such as the physically important minima of the instability boundary, are surprisingly insensitive to detailed microscopic properties of the considered form of matter.

Recently, Haskell *et al.* [21] illustrated how current X-ray and ultra-violet observations can constrain the physics of the r-mode instability. They discussed various mechanisms active in the interior of a neutron star and showed how these mechanisms can modify the instability window in order to be consistent with the observations.

The motivation of the present work, in view of the above studies, is to study extensively the nuclear equation of state (EOS) effect on the r-mode instability and evolution of neutron stars with a perfectly rigid crust [1, 18, 22, 23]. Actually EOS affects the time scales associated with the r-mode, in two different ways. Firstly, EOS defines the radial dependence of the mass density distribution $\rho(r)$, which is the basic ingredient of the relevant integrals (see Sec. II). Secondly, it defines the core-crust transition density ρ_c and also the core radius R_c which is the upper limit of the mentioned integrals. I employ a phenomenological model for the energy per baryon of the asymmetric nuclear matter having the advantage of an analytical form. By suitably choosing the parametrization of the model I obtain various forms for the density dependence of the nuclear symmetry energy by varying the slope parameter L in the interval $65 \text{ MeV} \leq L \leq 110 \text{ MeV}$. The calculated EOS concerns the neutron star core (from the center of the star up to the crust-core interface). For the neutron star crust I employed the EOS taken from the previous work of Feynman, Metropolis and Teller [24] and also from Baym, Pethick and Sutherland [25]. The transition pressure at the edge of the core is calculated by employing the thermodynamic method. It is found that in a good approximation the quantities connected with the r-mode instability are related directly with the slope parameter. The effects of the stiffness of EOS are studied on the gravitational and viscous time scales as well as on the critical angular velocity and critical temperature. I investigate the case whether the observed properties of the LMXBs and MSRPs should constrain the slope parameter L .

The interesting issue is how much the equation of state affects the time evolution of the frequency and spindown rate of a neutron star. This is also under consideration in the present work [26]. In particular, I develop my study on the evolution of r-mode by employing the mentioned EOS's and probing the sensitivity of the relevant quantities on the slope parameter L . A comparison of the theoretical predictions with a few observed cases is also presented and discussed.

It is worth pointing out that in the present study I do not include other additional dissipation mechanisms due for example to bulk and shear viscosity, which take into account the whole star and not only the boundary layer at the crust core transition. Actually, recently it was found that bulk and shear viscosities increase with L and therefore the damping of the mode is more efficient for the models with larger L [19]. In the present work I concentrate my study on the shear dissipation in the viscous boundary layer between crust and core. The mentioned dissipation mechanism decreases the viscous damping time scale by more than a factor of 10^5 in old, accreting neutron stars and more than 10^7 in hot young neutron stars and therefore becomes comparable to the gravitational radiation driving time scale [1, 15]. These cases efficiently limit the ability of the r-mode instability to reduce the angular momentum of the star and hence to produce detectable gravitational radiation [1].

The article is organized as follows. In Sec II I review briefly the stability and evolution of the r-modes. Section III contains the employed nuclear physics model focusing on the presentation of the nuclear symmetry energy and the thermodynamic method applied for location of core-crust interface. The results are presented and discussed in

Sec. IV and Sec. V summarizes the present study.

2 Stability and evolution of the r-modes

The r -modes evolve with a time dependence $e^{i\omega t - t/\tau}$ as a consequence of ordinary hydrodynamics and the influence of the various dissipative processes. The real part of the frequency of these modes, ω , is given by [27]

$$\omega = -\frac{(m-1)(m+2)}{m+1}\Omega, \quad (1)$$

where Ω is the angular velocity of the unperturbed star. The imaginary part $1/\tau$ is determined by the effects of gravitational radiation, viscosity, etc. [1, 27, 26]. In the small-amplitude limit, a mode is a driven, damped harmonic oscillator with an exponential damping time scale

$$\frac{1}{\tau(\Omega, T)} = \frac{1}{\tau_{GR}(\Omega)} + \frac{1}{\tau_{bv}(\Omega, T)} + \frac{1}{\tau_v(\Omega, T)}, \quad (2)$$

where τ_{GR} , τ_{bv} , τ_v are gravitational radiation, bulk viscosity and shear viscosity times scales respectively. Gravitational radiation tends to drive the r -modes unstable, while viscosity suppresses the instability. More precisely dissipative effects cause the mode to decay exponentially as $e^{-t/\tau}$ (i.e., the mode is stable) as long as $\tau > 0$ [27].

The damping time τ_i for the individual mechanisms is defined in general by [1, 19, 20]

$$\frac{1}{\tau_i} \equiv -\frac{1}{2E} \left(\frac{dE}{dt} \right)_i. \quad (3)$$

In Eq. (3) the total energy E of the r -mode is given by

$$E = \frac{1}{2}\alpha^2 R^{-2m+2}\Omega^2 \int_0^R \rho(r)r^{2m+2}dr, \quad (4)$$

where α is the dimensionless amplitude of the mode, R and Ω are the radius and the angular velocity of the neutron star respectively and $\rho(r)$ is the radial dependence of the mass density of the neutron star. Similar expressions hold for the dissipation rate $(dE/dt)_i$ [27].

The damping time scale due to viscous dissipation at the boundary layer of the perfectly rigid crust and fluid core is given by [1]

$$\tau_v = \frac{1}{2\Omega} \frac{2^{m+3/2}(m+1)!}{m(2m+1)!!\mathcal{I}_m} \sqrt{\frac{2\Omega R_c^2 \rho_c}{\eta_c}} \int_0^{R_c} \frac{\rho(r)}{\rho_c} \left(\frac{r}{R_c} \right)^{2m+2} \frac{dr}{R_c}, \quad (5)$$

where the quantities R_c , ρ_c and η_c are the radius, density and viscosity of the fluid at the outer edge of the core respectively. In deriving expression (5) it is assumed that the crust is rigid and hence static in the rotating frame. The motion of the crust due to the mechanical coupling to the core effectively increases τ_v by a factor of $(\Delta v/v)^{-2}$, where $\Delta v/v$ denotes the difference between the velocities in the inner edge of the crust and outer edge of the core divided by the velocity of the core [23].

In neutron stars colder than about 10^9 K the shear viscosity is expected to be dominated by electron-electron scattering. The viscosity associated with this process is given by [1]

$$\eta_{ee} = 6.0 \times 10^6 \rho^2 T^{-2}, \quad (\text{g cm}^{-1} \text{ s}^{-1}), \quad (6)$$

where all quantities are given in cgs units and T is measured in K. For temperature above 10^9 K, neutron-neutron scattering provides the dominant dissipation mechanism. In this range the viscosity is given by [1]

$$\eta_{nn} = 347 \rho^{9/4} T^{-2}, \quad (\text{g cm}^{-1} \text{ s}^{-1}). \quad (7)$$

In the present work I neglect the effects of bulk viscosity, which are not important for $T \leq 10^{10}$ K.

The fiducial viscous time scale $\tilde{\tau}_v$ is defined as

$$\tau_v = \tilde{\tau}_v \left(\frac{\Omega_0}{\Omega} \right)^{1/2} \left(\frac{T}{10^8 \text{ K}} \right), \quad (8)$$

where $\Omega_0 = \sqrt{\pi G \bar{\rho}}$ and $\bar{\rho} = 3M/4\pi R^3$ is the mean density of the star.

The gravitational radiation time scale is given by [1, 27]

$$\frac{1}{\tau_{GR}} = -\frac{32\pi G\Omega^{2m+2}}{c^{2m+3}} \frac{(m-1)^{2m}}{[(2m+1)!!]^2} \left(\frac{m+2}{m+1}\right)^{2m+2} \int_0^{R_c} \rho(r)r^{2m+2} dr, \quad (9)$$

while the fiducial gravitational radiation time scale $\tilde{\tau}_{GR}$ is defined as

$$\tau_{GR} = \tilde{\tau}_{GR} \left(\frac{\Omega_0}{\Omega}\right)^{2m+2}. \quad (10)$$

The critical angular velocity Ω_c , above which the r -mode is unstable, is defined by the condition $\tau_{GR} = -\tau_v$ and is given, for $m = 2$, by [1, 27]

$$\frac{\Omega_c}{\Omega_0} = \left(-\frac{\tilde{\tau}_{GR}}{\tilde{\tau}_v}\right)^{2/11} \left(\frac{10^8 K}{T}\right)^{2/11}. \quad (11)$$

For a given temperature T and mode m the equation for the critical angular velocity, that is $1/\tau(\Omega_c) = 0$, is a polynomial of order $m+1$ in Ω_c^2 , and thus each mode has its own critical angular velocity [27]. However, only the smallest of these (the $m = 2$ r-mode here) represents the critical angular velocity of the star and I concentrate my study on this r-mode.

Moreover, the maximum angular velocity Ω_K (Kepler angular velocity) for any star occurs when the material at the surface effectively orbits the star [27]. This velocity is nearly $\Omega_K = \frac{2}{3}\Omega_0$. Thus, there is a critical temperature below which the gravitational radiation instability is completely suppressed by viscosity and is given by [1]

$$\frac{T_c}{10^8 K} = \left(\frac{\Omega_0}{\Omega_c}\right)^{11/2} \left(-\frac{\tilde{\tau}_{GR}}{\tilde{\tau}_v}\right) = \left(\frac{3}{2}\right)^{11/2} \left(-\frac{\tilde{\tau}_{GR}}{\tilde{\tau}_v}\right). \quad (12)$$

Employing Eqs. (11) and (12) the critical angular velocity is expressed in terms of T_c , that is

$$\frac{\Omega_c}{\Omega_0} = \frac{\Omega_K}{\Omega_0} \left(\frac{T_c}{T}\right)^{2/11} = \frac{2}{3} \left(\frac{T_c}{T}\right)^{2/11}. \quad (13)$$

Once the equation of state for the neutron star core and crust is fixed, then all the ingredients of the r-mode instability, that is the transition density ρ_c , the radial dependence of the mass density $\rho(r)$, and the bulk properties of the neutron star (mass, radius and core radius) are determined in a self-consistent way.

Following the discussion of Owen *et al.* [26] during the phase where the angular momentum is radiated away to infinity by gravitational radiation, the angular velocity evolves as follows

$$\frac{d\Omega}{dt} = \frac{2\Omega}{\tau_{GR}} \frac{\alpha^2 Q}{1 - \alpha^2 Q}, \quad (14)$$

where α is the dimensionless r-mode amplitude parameter. In general, α which strongly affects the r-mode evolution is treated as a free parameter and usually varied on the large interval $\alpha = 1 - 10^{-8}$. The quantity Q related with the equation of state is defined as $Q = 3\tilde{J}/2\tilde{I}$ where

$$\tilde{J} = \frac{1}{MR^4} \int_0^R \rho(r)r^6 dr, \quad \tilde{I} = \frac{8\pi}{2MR^2} \int_0^R \rho(r)r^4 dr. \quad (15)$$

In order to complete the model for the evolution of the r-mode, one may take into account the thermal evolution, since temperature strongly influences the dissipation mechanisms. The mentioned thermal evolution can be studied with an energy balance between the relevant radiative and viscous process, that is [2]

$$\frac{dT}{dt} = \frac{1}{C_v} (-L_\nu + H_s). \quad (16)$$

In Eq. (16) L_ν is the neutrino luminosity, H_s is the heating rate generated by shear viscosity and C_v is the total heat capacity. In the present work, I consider the approximate case where the heating process balances the cooling one, that is $L_\nu = H_s$ (for a more detailed analysis see Ref. [28]). In this simplified case the solution of Eq. (14) gives

$$\Omega(t) = \left(\frac{1}{\Omega_{in}^{-6} - Ct}\right)^{1/6}, \quad (17)$$

where

$$C = \frac{2\alpha^2 Q}{\tilde{\tau}_{GR}(1 - \alpha^2 Q)} \frac{1}{\Omega_0^6}. \quad (18)$$

Ω_{in} is a free parameter which corresponds to the initial angular velocity. The spindown rate of the angular velocity can be easily derived from Eq. (17) and is given by

$$\frac{d\Omega}{dt} = \frac{\mathcal{C}}{6} \left(\frac{1}{\Omega_{in}^{-6} - \mathcal{C}t} \right)^{7/6}. \quad (19)$$

A neutron star spin decreases until it approaches its critical angular velocity Ω_c . The time t_c needed for Ω_{in} to evolve to its minimum value Ω_c is

$$t_c = \frac{1}{\mathcal{C}} (\Omega_{in}^{-6} - \Omega_c^{-6}). \quad (20)$$

3 The nuclear model

The model used here, which has already been presented and analyzed in previous papers [29, 30, 31, 32, 33, 34], is designed to reproduce the results of the microscopic calculations of both nuclear and neutron-rich matter at zero temperature and can be extended to finite temperature [29, 31, 32, 33, 34]. The energy per baryon at $T = 0$, is given by

$$\begin{aligned} E_b(n, I) &= \frac{3}{10} E_F^0 u^{2/3} \left[(1+I)^{5/3} + (1-I)^{5/3} \right] + \frac{1}{3} A \left[\frac{3}{2} - \left(\frac{1}{2} + x_0 \right) I^2 \right] u \\ &+ \frac{\frac{2}{3} B \left[\frac{3}{2} - \left(\frac{1}{2} + x_3 \right) I^2 \right] u^\sigma}{1 + \frac{2}{3} B' \left[\frac{3}{2} - \left(\frac{1}{2} + x_3 \right) I^2 \right] u^{\sigma-1}} \\ &+ \frac{3}{2} \sum_{i=1,2} \left[C_i + \frac{C_i - 8Z_i I}{5} \right] \left(\frac{\Lambda_i}{k_F^0} \right)^3 \left(\frac{((1+I)u)^{1/3}}{\frac{\Lambda_i}{k_F^0}} - \tan^{-1} \frac{((1+I)u)^{1/3}}{\frac{\Lambda_i}{k_F^0}} \right) \\ &+ \frac{3}{2} \sum_{i=1,2} \left[C_i - \frac{C_i - 8Z_i I}{5} \right] \left(\frac{\Lambda_i}{k_F^0} \right)^3 \left(\frac{((1-I)u)^{1/3}}{\frac{\Lambda_i}{k_F^0}} - \tan^{-1} \frac{((1-I)u)^{1/3}}{\frac{\Lambda_i}{k_F^0}} \right). \end{aligned} \quad (21)$$

In Eq. (21), I is the asymmetry parameter ($I = (n_n - n_p)/n$) and $u = n/n_0$, with n_0 denoting the equilibrium symmetric nuclear matter density, $n_0 = 0.16 \text{ fm}^{-3}$. The parameters A , B , σ , C_1 , C_2 and B' which appear in the description of symmetric nuclear matter are determined in order that $E_b(n = n_0, I = 0) = -16 \text{ MeV}$, $n_0 = 0.16 \text{ fm}^{-3}$, and the incompressibility is $K = 240 \text{ MeV}$ and have the values $A = -46.65$, $B = 39.45$, $\sigma = 1.663$, $C_1 = -83.84$, $C_2 = 23$ and $B' = 0.3$. The finite range parameters are $\Lambda_1 = 1.5k_F^0$ and $\Lambda_2 = 3k_F^0$ and k_F^0 is the Fermi momentum at the saturation point n_0 . The baryon energy is written also as a function of the baryon density n and the proton fraction x ($x = n_p/n$), that is $E_b(n, x)$, by replacing $I = 1 - 2x$.

The additional parameters x_0 , x_3 , Z_1 , and Z_2 employed to determine the properties of asymmetric nuclear matter are treated as parameters constrained by empirical knowledge [29]. The parameterizations used in the present model have only a modest microscopic foundation. Nonetheless, they have the merit of being able to closely approximate more physically motivated calculations as presented in Fig. 1. More precisely, in Fig. 1 I compare the energy per baryon (for symmetric nuclear matter (Fig. 1a) and pure neutron matter (Fig. 1b)) calculated by the present schematic model referred to as momentum-dependent interaction model (MDIM), with those of existing, state of the art calculations by Wiringa et al. [35] and Pandharipande et al. [36].

3.1 Symmetry energy

The energy $E_b(n, I)$ can be expanded around $I = 0$ as follows

$$E_b(n, I) = E_b(n, I = 0) + E_{sym,2}(n)I^2 + E_{sym,4}(n)I^4 + \dots + E_{sym,2k}(n)I^{2k} + \dots, \quad (22)$$

where the coefficients of the expansion are given by the expression

$$E_{sym,2k}(n) = \frac{1}{(2k)!} \left. \frac{\partial^{2k} E_b(n, I)}{\partial I^{2k}} \right|_{I=0}. \quad (23)$$

In (22), only even powers of I appear due to the fact that the strong interaction must be symmetric under exchange of neutrons with protons i.e. the contribution to the energy must be independent of the sign of the difference $n_n - n_p$. The nuclear symmetry energy $E_{sym}(n)$ is defined as the coefficient of the quadratic term, that is

$$E_{sym}(n) = E_{sym,2}(n) = \frac{1}{2!} \left. \frac{\partial^2 E_b(n, I)}{\partial I^2} \right|_{I=0}. \quad (24)$$

The slope of the symmetry energy L at nuclear saturation density n_0 , which is correlated with the crust-core transition density n_t in a neutron star, is defined as

$$L = 3n_0 \left. \frac{dE_{sym}(n)}{dn} \right|_{n=n_0}. \quad (25)$$

By suitably choosing the parameters x_0 , x_3 , Z_1 , and Z_2 , it is possible to obtain different forms for the density dependence of the symmetry energy $E_{sym}(n)$ as well as on the value of the slope parameter L . I take as a range of L $65 \text{ MeV} \leq L \leq 110 \text{ MeV}$ where the value of the symmetry energy at saturation density is fixed to be $E_{sym}(n_0) = 30 \text{ MeV}$. Actually, for each value of L the density dependence of the symmetry energy is adjusted so that the energy of pure neutron matter is comparable with those of existing state-of-the-art calculations [35, 36].

Fig. 2(a) displays the behavior of the nuclear symmetry energy as a function of the ratio $u = n/n_0$ for various values of the slope parameter L . The aim of the above simple parametrization is to reproduce the nuclear symmetry energy originating from more realistic microscopic calculations and also covers the possible range of the nuclear symmetry energy dependence on the density.

3.2 Proton fraction

I examine the proton fraction x (as a function of the baryon density n) in β -stable matter. In this case the following processes take place simultaneously

$$n \longrightarrow p + e^- + \bar{\nu}_e \quad p + e^- \longrightarrow n + \nu_e, \quad (26)$$

I assume that neutrinos generated in these reactions have left the system. This implies that

$$\hat{\mu} = \mu_n - \mu_p = \mu_e. \quad (27)$$

The demand for equilibrium leads to equation

$$\frac{\partial}{\partial x} \left(E_b(n, x) + E_e(n, x) \right) = 0, \quad (28)$$

or

$$\left(\frac{\partial E_b}{\partial x} \right)_n = - \left(\frac{\partial E_e}{\partial x} \right)_n = -\mu_e. \quad (29)$$

Finally, considering that the chemical potential of the electron is given by the relation (relativistic electrons)

$$\mu_e = \sqrt{k_{F_e}^2 c^2 + m_e^2 c^4} \simeq k_{F_e} c = \hbar c (3\pi^2 n x)^{1/3}, \quad (30)$$

then Eq. (29) is written

$$\left(\frac{\partial E_b}{\partial x} \right)_n = -\hbar c (3\pi^2 n x)^{1/3}. \quad (31)$$

Eq. (31) determines the proton fraction of β -stable matter. In Fig. 2(b) I plot the proton fraction calculated from equation (31) as a function of the ratio $u = n/n_0$ for various values of the slope parameter L . According to Fig. 2(b) for low values of L , the neutron star matter consists mainly from neutrons and only a very small fraction of protons. However the increase of L (and consequently the increase of the stiffness of EOS) leads to an increase of the proton fraction. The values of the proton fraction define the kind of the cooling process of a hot neutron star. More precisely, it is well known that the direct Urca process can occur in neutron stars if the proton concentration exceeds the critical value $x_{crit} = 0.11$ for neutron star matter with electrons and $x_{crit} = 0.148$ when electrons and muons coexist in neutron star matter [37].

3.3 Nuclear equation of state for β -stable matter

The total pressure $P(n, x)$, in the core of a neutron star, is decomposed into baryon and electron contributions

$$P(n, x) = P_b(n, x) + P_e(n, x), \quad (32)$$

where

$$P_b(n, x) = n^2 \frac{\partial E_b(n, x)}{\partial n}. \quad (33)$$

The electrons are considered as a non-interacting relativistic Fermi gas and their contribution to the total energy density $\epsilon_e(n, x)$ and pressure $P_e(n, x)$ reads

$$\epsilon_e(n, x) = \frac{\hbar c}{4\pi^2} (3\pi^2 x n)^{4/3}, \quad (34)$$

$$P_e(n, x) = \frac{\hbar c}{12\pi^2} (3\pi^2 x n)^{4/3}. \quad (35)$$

Now the total energy density ϵ_{tot} and pressure P_{tot} of charge neutral and chemically equilibrium nuclear matter is

$$\epsilon_{tot} = \epsilon_b + \epsilon_e, \quad (36)$$

$$P_{tot} = P_b + P_e. \quad (37)$$

From Eqs. (36) and (37) I construct the equation of state in the form $\epsilon = \epsilon(P)$. When the electrons energy is large enough (i.e. greater than the muon mass), it is energetically favorable for the electrons to convert to muons

$$e^- \longrightarrow \mu^- + \bar{\nu}_\mu + \nu_e. \quad (38)$$

However, in the present work I will not include the muon case to the total equation of state since the muon contribution does not alter significantly the gross properties of the neutron stars.

3.4 The thermodynamical method

The core-crust interface corresponds to the phase transition between nuclei and uniform nuclear matter. The uniform matter is nearly pure neutron matter, with a proton fraction of just a few percent determined by the condition of beta equilibrium. Weak interactions conserve both baryon number and charge [38], and from the first law of thermodynamics, at temperature $T = 0$ I have

$$d\mathcal{E} = -Pdv - \hat{\mu}dq, \quad (39)$$

where \mathcal{E} is the internal energy per baryon, P is the total pressure, v is the volume per baryon ($v = 1/n$ where n is the baryon density) and q is the charge fraction ($q = x - Y_e$ where x and Y_e are the proton and electron fractions in baryonic matter respectively). In β -equilibrium the chemical potential $\hat{\mu}$ is given by $\hat{\mu} = \mu_n - \mu_p = \mu_e$ where μ_p , μ_n and μ_e are the chemical potentials of the protons, neutrons and electrons respectively. The stability of the uniform phase requires that $\mathcal{E}(v, q)$ is a convex function [39]. This condition leads to the following two constraints for the pressure and the chemical potential

$$-\left(\frac{\partial P}{\partial v}\right)_q - \left(\frac{\partial P}{\partial q}\right)_v \left(\frac{\partial q}{\partial v}\right)_{\hat{\mu}} > 0, \quad (40)$$

$$-\left(\frac{\partial \hat{\mu}}{\partial q}\right)_v > 0. \quad (41)$$

It is assumed that the total internal energy per baryon $\mathcal{E}(v, q)$ can be decomposed into baryon (E_N) and electron (E_e) contributions

$$\mathcal{E}(v, q) = E_b(v, q) + E_e(v, q). \quad (42)$$

The relative theory has been extensively presented in the recent publication [40]. I consider the condition of charge neutrality $q = 0$ which requires that $x = Y_e$. This is the case which will also be taken into account in the present study. Hence, according to Ref. [40] the constraints (40) and (41), after some algebra lead to the following constraint

$$C(n) = 2n \frac{\partial E_b(n, x)}{\partial n} + n^2 \frac{\partial^2 E_b(n, x)}{\partial n^2} - \left(\frac{\partial^2 E_b(n, x)}{\partial n \partial x} n\right)^2 \left(\frac{\partial^2 E_b(n, x)}{\partial x^2}\right)^{-1} > 0, \quad (43)$$

For a given equation of state, the quantity $C(n)$ is plotted as a function of the baryon density n and the equation $C(n) = 0$ defines the transition density n_t .

4 Results and Discussion

I employ a phenomenological model for the energy per baryon of the asymmetric nuclear matter having the advantage of an analytical form. By suitably choosing the parametrization of the model I obtain various forms for the density dependence of the energy per baryon of neutron matter (see Fig. 1(b)), the nuclear symmetry energy (see Fig. 2(a)) and the proton fraction (see Fig. 2(b)), and in total the neutron star core equation of state.

In order to clarify further the effect of the symmetry energy on the proton fraction I plot in Fig. 2(c) the density dependence of the fourth order term $E_{sym,4}(n)$ (see the expansion (22)) for the various values of L . Considering, for example a fourth order approximation on the symmetry energy and combining Eqs. (31) and (22) I found that the density dependence of the proton fraction is determined by the equation

$$4(1 - 2x)E_{sym,2}(n) + 8(1 - 2x)^3 E_{sym,4}(n) \simeq \hbar c(3\pi^2 nx)^{1/3}.$$

Obviously, the second order term $E_{sym,2}(n)$ mostly affects the proton fraction density dependence. However, the contribution of the fourth order term $E_{sym,4}(n)$ is not negligible and in some cases (see for example the case $L = 65$) has a significant effect on $x(n)$.

Additionally, the present model is applied for the determination of the transition density n_t between the crust and the core. In order to complete the equation of state which describes the neutron star matter for densities lower than the transition density n_t (equation of state of the crust) I employed the relative equation of state of Feynman, Metropolis and Teller [24] and also of Baym, Pethick and Sutherland [25].

In Fig. 3(a), I plot the transition density n_t , which is a fundamental quantity in the present study, as a function of the slope parameter L . A linear relation is found of the form

$$n_t = 0.1253 - 0.0007 L \text{ (fm}^{-3}\text{)}, \quad (44)$$

where the slope parameter L is given in MeV. According to relation (44) an increase of L (a stiffer equation of state) leads to a decrease of n_t , to the extension of both the total radius R (since the mass is fixed) and the radius core R_c . In Fig. 3(b), I plot also the dependence of the transition pressure P_t on L . Actually, during the last years there is an extensive interest for the study of the transition density and pressure in neutron stars [40, 41, 42, 43]. It was found that the transition density and pressure decrease roughly linearly with the slope parameter L using dynamical and thermodynamical methods [40, 41]. The authors in Refs. [42, 43] used a large number of nuclear models and evaluated the dispersion affecting the correlation between the transition pressure P_t and L . From a detailed analysis it was shown that this correlation is weak but P_t is mainly correlated with the symmetry energy slope L and curvature K_{sym} defined at $\rho = 0.1 \text{ fm}^{-3}$ [42, 43].

The transition pressure does not affect directly the time scales corresponding to the r-mode instability. However it influences significantly the crustal fraction of the moment of inertia $\Delta I/I$ [44]. The ratio $\Delta I/I$ is particularly interesting as it can be inferred from observations of pulsar glitches that is occasional disruptions of the otherwise extremely regular pulsations from magnetized, rotating neutron stars [41].

In Fig. 4 I display the energy density E_{ns} of neutron star matter, including both the fluid core and the solid crust matter, as a function of the pressure P for various values of the slope parameter L . The mentioned equations of state are employed in order to solve the Tolman-Oppenheimer-Volkoff equations to calculate the bulk neutron star properties that is the mass, radius, density distribution of the baryonic matter e.t.c. which are the basic "ingredients" for the study of the r-mode instability and evolution.

In Fig. 5 I display the mass-radius relation for neutron stars for the selected equation of states. All of them predict maximum mass for neutron stars even higher than $1.8M_\odot$. To further illustrate the mass-radius relation I present in Table I and II the transition density n_t , transition pressure P_t , the total radius of the star R , the core radius R_c , the core mass M_c as well as the central pressure P_c for various values of the parameter L for neutron star mass $1.4M_\odot$ and $1.8M_\odot$ respectively .

Considering that $\epsilon(r)$ is the energy density function defined as $\epsilon(r) = \rho(r)/c^2$, then the integral $\int_0^{R_c} \rho(r)r^6 dr$, which is a basic ingredient of the r-mode energy E given by Eq. (4) and also of the time scales (Eqs. (5) and (9) respectively), can be written in the dimensionless form

$$I(R_c) = \int_0^{R_c} \left(\frac{\epsilon(r)}{\text{MeV fm}^{-3}} \right) \left(\frac{r}{\text{km}} \right)^6 d \left(\frac{r}{\text{km}} \right).$$

The integral $I(R_c)$ is plotted in Fig. 6, as a function of the slope parameter L for the interval $72.5 \text{ MeV} \leq L \leq 110 \text{ MeV}$. It is obvious that the values of $I(R_c)$ are correlated almost linearly with L in the considered interval. The least-squares fit expressions are respectively

$$I(R_c) = \left(0.7 + 0.084L \right) 10^8, \quad (M = 1.4M_\odot) \quad (45)$$

$$I(R_c) = \left(1.24 + 0.0845L \right) 10^8, \quad (M = 1.8M_\odot) \quad (46)$$

where the slope parameter L is given in MeV.

The fiducial gravitational radiation time scale $\tilde{\tau}_{GR}$ combining Eqs. (9) and (10) and after some algebra takes the form

$$\tilde{\tau}_{GR} = -0.7429 \left(\frac{R}{\text{km}} \right)^9 \left(\frac{1M_\odot}{M} \right)^3 [I(R_c)]^{-1} \text{ (sec)}, \quad (47)$$

where R, r are given in km and M in M_\odot . I can proceed further by putting Eq. (45) into (47). In this way the time scale $\tilde{\tau}_{GR}$ corresponds to a neutron star with mass $1.4 M_\odot$ given by the simple expression

$$\tilde{\tau}_{GR} = -2.70736 \left(\frac{R}{10\text{km}} \right)^9 \frac{1}{0.7 + 0.084L} \text{ (sec)}. \quad (48)$$

It is worth to point out that $\tilde{\tau}_{GR}$, according to Eq. (48) depends directly on the slope parameter L , as well as indirectly on the values of the radius R . In any case, Eq. (48) exhibits the equation of state dependence of the time scale $\tilde{\tau}_{GR}$ in a quantitative way.

As a first approximation I can consider the case where the mass density of the neutron star $\rho(r)$ is uniform that is $\rho(r) = \bar{\rho} \equiv 3M/4\pi R^3$. Actually, this case is unphysical because the energy density does not vanish on the surface and the speed of sound $c_s = \sqrt{\partial P/\partial \rho}$ is infinite [45]. However, I consider this case since it has been extensively applied for r-mode instabilities studies. After some algebra $\tilde{\tau}_{GR}^{approx}$ is written

$$\tilde{\tau}_{GR}^{approx} = -1.95 \left(\frac{R}{10\text{km}} \right)^{12} \left(\frac{10\text{km}}{R_c} \right)^7 \left(\frac{1M_\odot}{M} \right)^4 \text{ (sec)}. \quad (49)$$

In Fig. 7, as well as in Table III, I compare the values of $\tilde{\tau}_{GR}$ and $\tilde{\tau}_{GR}^{approx}$. Actually both are increasing functions of the slope parameter L , for low values of L , but for higher values show a saturation trend. The approximated values for gravitational time scales are lower between 8% – 16% (for $M = 1.4M_\odot$) and lower by 23% – 28% (for $M = 1.8M_\odot$). Consequently, the mean density approximation, concerning the gravitational time scales works better for low neutron star mass values.

The fiducial viscous time $\tilde{\tau}_v$ which results from Eqs. (5), (6), (7) and (8) after some algebra is written for the case of viscosity due to electron-electron and neutron-neutron scattering respectively

$$\tilde{\tau}_{ee} = 0.1446 \cdot 10^8 \left(\frac{R}{\text{km}} \right)^{3/4} \left(\frac{1M_\odot}{M} \right)^{1/4} \left(\frac{\text{km}}{R_c} \right)^6 \left(\frac{\text{gr cm}^{-3}}{\rho_c} \right)^{1/2} \left(\frac{\text{MeV fm}^{-3}}{\epsilon_c} \right) I(R_c) \text{ (sec)}, \quad (50)$$

$$\tilde{\tau}_{nn} = 19 \cdot 10^8 \left(\frac{R}{\text{km}} \right)^{3/4} \left(\frac{1M_\odot}{M} \right)^{1/4} \left(\frac{\text{km}}{R_c} \right)^6 \left(\frac{\text{gr cm}^{-3}}{\rho_c} \right)^{5/8} \left(\frac{\text{MeV fm}^{-3}}{\epsilon_c} \right) I(R_c) \text{ (sec)} \quad (51)$$

where ρ_c and ϵ_c are the mass density (in gr cm^{-3}) and the energy density (in MeV fm^{-3}) respectively at the core edge. It is found that an almost linear relation holds between the mass transition density ρ_c and the slope parameter L (and consequently a similar relation between ϵ_c and L), for the interval $72.5 \text{ MeV} \leq L \leq 110 \text{ MeV}$, with the form

$$\rho_c = \left(2.148 - 0.0125L \right) \times 10^{14} \text{ (gr} \cdot \text{cm}^{-3}), \quad (52)$$

$$\epsilon_c = \left(2.148 - 0.0125L \right) \times 56.1837 \text{ (MeV} \cdot \text{fm}^{-3}). \quad (53)$$

Combining Eqs. (50), (51) (52) and (53) I found for a neutron star mass with $M = 1.4M_\odot$ and for the interval ($72.5 \text{ MeV} \leq L \leq 110 \text{ MeV}$), the simple expressions

$$\tilde{\tau}_{ee} = 13.3053 \left(\frac{R}{10\text{km}} \right)^{3/4} \left(\frac{10\text{km}}{R_c} \right)^6 \frac{0.7 + 0.084L}{(2.148 - 0.0125L)^{3/2}} \text{ (sec)} \quad (M = 1.4M_\odot) \quad (54)$$

$$\tilde{\tau}_{nn} = 31.09 \left(\frac{R}{10\text{km}} \right)^{3/4} \left(\frac{10\text{km}}{R_c} \right)^6 \frac{0.7 + 0.084L}{(2.148 - 0.0125L)^{13/8}} \text{ (sec)} \quad (M = 1.4M_\odot). \quad (55)$$

By employing the mean density approximation the corresponding expressions are

$$\tilde{\tau}_{ee}^{approx} = 55.1657 \left(\frac{10\text{km}}{R} \right)^{9/4} \left(\frac{R_c}{10\text{km}} \right) \left(\frac{M}{1M_\odot} \right)^{3/4} \left(\frac{\text{gr} \cdot \text{cm}^{-3}}{\rho_{c,14}} \right)^{3/2} \text{ (sec)} \quad (56)$$

$$\tilde{\tau}_{nn}^{approx} = 129 \left(\frac{10\text{km}}{R} \right)^{9/4} \left(\frac{R_c}{10\text{km}} \right) \left(\frac{M}{1M_\odot} \right)^{3/4} \left(\frac{\text{gr} \cdot \text{cm}^{-3}}{\rho_{c,14}} \right)^{13/8} \quad (\text{sec}), \quad (57)$$

where $\rho_{c,14}$ is given in $10^{14}\text{gr} \cdot \text{cm}^{-3}$. In Fig. 7, as well as in Table III, I compare the fiducial viscous time scales. Both time scales are an increasing function of the slope parameter L , that is a stiffer equation of state leads to smaller viscosity effects on the r-mode. The approximated values for the viscosity timescales are between 9% – 16% (for $M = 1.4M_\odot$) and between 23% – 28% (for $M = 1.8M_\odot$). Consequently, the mean density approximation, concerning the viscosity time scales, works better for low values of neutron stars.

In Fig. 8 are displayed the r-mode instability windows (which specified by the Ω_c/Ω_0 - T dependence) for neutron stars with mass $1.4M_\odot$ and $1.8M_\odot$ for the selected equations of state as a function of the temperature. For low values of temperature ($T \leq 10^9$ K) I plot the ratio

$$\frac{\Omega_c}{\Omega_0} = \left(-\frac{\tilde{\tau}_{GR}}{\tilde{\tau}_{ee}} \right)^{2/11} \left(\frac{10^8 \text{ K}}{T} \right)^{2/11}, \quad (58)$$

while for $T \geq 10^9$ K I plot the ratio

$$\frac{\Omega_c}{\Omega_0} = \left(-\frac{\tilde{\tau}_{GR}}{\tilde{\tau}_{nn}} \right)^{2/11} \left(\frac{10^8 \text{ K}}{T} \right)^{2/11}. \quad (59)$$

The most striking feature is the location of the ratio Ω_c/Ω_0 in a narrow interval (mainly in the case of neutron star with mass $1.4M_\odot$). Actually, the ratio Ω_c/Ω_0 increases around 7.7% (for $T \leq 10^9$ K) and around 8.7% (for $T \geq 10^9$ K) with the lower values corresponding to the case of $L = 110$ MeV and the higher to the case $L = 80$ MeV. It is concluded that the values of that ratio saturate for L close to the value 80 MeV. In the case of a neutron star with mass $M = 1.8M_\odot$ the ratio Ω_c/Ω_0 increases around 5.5% (for $T \leq 10^9$ K) and around 6.5% (for $T \geq 10^9$ K) with the lower values corresponding to the case of $L = 110$ MeV and the higher to the case $L = 80$ MeV.

Moreover I study the effect of the nuclear equation of state on Ω_c . In particular, I examine the sensitivity of Ω_c on the density dependence of symmetry energy. Thus, by combining Eqs. (47), (50) and (58), for a fixed neutron star mass and temperature, I found the relation

$$\Omega_c \sim \frac{R_c^{12/11}}{(I(R_c))^{4/11}} \rho_c^{3/11}. \quad (60)$$

It is obvious, from Eq. (60), that Ω_c is sensitive to the structure (due to the factor $I(R_c)$), size (due to R_c) and the interface edge (due to ρ_c) of the core of the neutron star. Consequently, Ω_c is sensitive both to the high density dependence of the EOS via the factors R_c and $I(R_c)$ as well as to the low density dependence of the symmetry energy via the factor ρ_c . In addition, and summing up it is shown that Ω_c is inversely proportional to the core radius R_c (the higher value of L the lower is the value of Ω_c) and proportional to $\rho_c^{3/11}$ (a higher values of L corresponds to a lower values of ρ_c). It is worthwhile to notice here that the dependence of ρ_c on the slope parameter L is model dependent. It has been found recently that the error due to the assumption that a priori the equation of state is parabolic may introduce a large error in the determination of related properties of neutron stars as the crustal fraction of the moment of inertia and the critical frequency of rotating neutron stars [41, 46].

The critical temperature T_c , defined by Eq. (12), is plotted in Fig. 9, as a function of the slope parameter L for neutron star with mass $1.4M_\odot$ and $1.8M_\odot$. T_c is in the range from 0.73×10^8 to 1.1×10^8 K (for $1.4M_\odot$ neutron star mass) and from 0.18×10^8 to 0.24×10^8 (for $1.8M_\odot$ neutron star mass) where the maximum values of T_c correspond to equation of state with $L = 80$ MeV. In particular, T_c is a decreasing function of L (for $L \geq 80$ MeV). The present finding is in contradiction with the corresponding one presented in Ref. [18] where T_c is a monotonously increasing function of L for a large interval ($25 \leq L \leq 105$ MeV). The above disagreement may be attributed with the use of two different models. More precisely, T_c , according to Eq. (12), depends on the interplay between $\tilde{\tau}_{GR}$ and $\tilde{\tau}_{ee}$, and consequently, for fixed neutron star mass, on the parameter L . Obviously, this interplay is model dependent and related with the L dependence on the fiducial times scales as exhibited in Fig. 7 of the present work and in Fig. 3 of Ref. [18]. Although, in contrast to T_c - L dependence the present results are quantitatively in very good agreement with those in Ref. [18], at least for the $1.4M_\odot$ neutron star mass and for the same range of L .

In Fig. 10 I compare the r-mode instability window for the selected equations of state with those of the observed neutron stars in LMXBs and MSRPs for $M = 1.4M_\odot$ and $M = 1.8M_\odot$. I find that the instability window drops by $\simeq 20 - 40$ Hz when the mass is raised from $M = 1.4M_\odot$ to $M = 1.8M_\odot$. In addition, the stiffness equation of state leads an increase of the instability window (which specified, in this case, by the ν_c - T dependence). Following the study of Wen *et al.* [18] and Haskell *et al.* [21] I include many cases of LMXBs and a few of MSRPs (for more details see [47, 48] and Table 1 of Ref. [21]). The masses of the mentioned stars are not measured accurately. In addition, it is worth pointing out that the estimates of the core temperature have large uncertainties. In the

present work, the core temperatures T are taken from Ref. [21] and the uncertainties, in a few relevant cases, are derived by employing the method suggested in Ref. [49]. In particular, the core temperatures T are derived by combining their observed accretion luminosity and considering that the cooling is dominated by the modified Urca neutrino process for normal nucleons (lower limit of T) or by the modified Urca, taking into account the effect of the superfluid neutrons and superconductive protons on the neutron star core (upper limit of T).

It is obvious from Fig. 10 that the majority of the stars lie outside the instability windows predicted by the present model. There are four exceptions, that is the *4U 1608-52*, the *SAX J1750.8-2900*, the *4U-1636-536* and the *MXB 1658-298*. Obviously, the above stars lie inside the instability window for the case of neutron star mass $M = 1.4M_\odot$ and $M = 1.8M_\odot$. The present results are comparable but not similar with those in Ref. [18] and in contradiction with those presented in Refs. [19] and [21]. More precisely, in Ref. [18] the authors employed a simple phenomenological model of a neutron star with a perfectly rigid crust, as mentioned in the Introduction and they concluded that, at least, for the case of low neutron star mass $M = 1.4M_\odot$, a softer EOS increases the lower frequency bound of the instability window and therefore the EOSs characterized by $L \leq 65$ MeV are more consistent with the observation of various LMXBs frequencies. The model employed in the present work predicts an even larger instability region, compared to Ref. [18] both for low and high values of neutron star mass. This is the reason that even for the case $M = 1.4M_\odot$ four neutron stars lie inside the instability window in contrast with the finding of Ref. [18]. In any case, the main conclusion of the two models is summarized as follows: the stiffness of the equation of state has a strong effect on the width of the instability window and this effect is more pronounced for high values of the neutron star mass.

On the other hand the author in Ref. [19], using various microscopic and phenomenological approaches, found that the r-mode instability region is smaller for those models which give larger values of L . The explanation is related with the L dependence of the bulk and the shear viscosities. In particular, the author found that both bulk and shear viscosities increase with L and consequently, damping of the r-mode is more efficient for models with larger L . In the present work, I consider that, in contradiction with the study of Ref. [19], the damping mechanism is due only to viscous dissipation at the boundary layer of perfectly rigid crust and fluid core (the study in Ref. [18], is based in the same consideration). The relative viscosity (given by Eqs. (6) and (7)) is fixed to the crust-core interface region and is proportional to the transition density. Thus, it is obvious by using relation (44) as well, that the viscosity is a decreasing function of L . The L dependence of the viscosity is well reflected on the values of the fiducial time scales $\tilde{\tau}_{ee}$ and $\tilde{\tau}_{nn}$ (see Eq.(5) and consequently on the values of the critical angular momentum and frequency (according to Eq.(11)) as exhibited in Fig. 10.

Moreover, in [21] the authors by employing the "minimal model", found that a significant number of systems is well inside the instability window. A possible explanation of the mentioned contradiction is the viscous dissipation at the boundary layer between crust and core, which is taken into account explicitly in the present work. Actually, when the authors in Ref. [21] include the above dissipation mechanism via the "slip" parameter S [50] (related with the rigidity of the crust) the majority of the stars *shifted* to the stability area in accordance with the observations, since the majority of the LMXBs should be out of the instability window (see also Refs. [51, 52]).

I extend also my study on the effect of the isoscalar part of the EOS to the critical rotational frequency ν_c . The incompressibility K , which is one of the main quantities related directly with the isoscalar behavior of the EOS, is defined as

$$K = 9n^2 \left. \frac{d^2(E/A)}{d^2n} \right|_{n=n_0} \quad (\text{MeV}), \quad (61)$$

where E/A is the energy per particle of symmetric nuclear matter and n_0 the saturation density. The parametrization of E/A is given in Table 2 of Ref. [29]. In particular, I kept fixed the nuclear symmetry dependence, and varied the incompressibility in a large range of $K = 180 - 240$ MeV according to the method presented in Ref. [29]. In this case, the energy per particle of symmetric nuclear matter is given by Eq. (21) and the symmetry energy by the simple analytical formula

$$E_{sym}(u) = 13u^{2/3} + 17u \quad (\text{MeV}). \quad (62)$$

The value of the slope parameter L , corresponding to the above ansatz of the symmetry energy, is $L = 77$ MeV. The results are presented in Fig. 11. A stiffer equation of state (higher values of K) leads to lower values of ν_c . The critical frequency decreases by around 7% for $K = 120$ MeV to $K = 240$ MeV. Obviously, the effect of K on ν_c is moderate, compared to the effect of the slope parameter L , but not negligible. However, since the most experimental values of K are well constrained around the value 240 MeV, the uncertainty related with the isoscalar effects on the equation of state and consequently on the critical frequency is limited.

The equation of state affects not only the conditions for the r-mode instability but also the angular velocity evolution of a neutron star according to Eq. (14). Actually, the quantities Q and τ_{GR} depend mainly on the density distribution as well as on the bulk neutron star properties as the mass and radius. I examine the approximated case of the frequency evolution considering thermal stability. More precisely I consider a neutron star with mass $M = 1.4M_\odot$, temperature $T = 8 \cdot 10^8$ K, initial frequency $\nu_{in} = 700$ Hz and r-mode amplitude $\alpha = 2 \cdot 10^{-7}$. The

results are presented in Fig. 12. It is worth pointing out that the value of Q moderately depends on the use of a specific equation of state and varies in the interval $Q = 0.0945 - 0.0977$. The equation of state affects mainly the time scale τ_{GR} . In Fig. 12(a) is displayed the time evolution of the frequency of a neutron star for the five EOSs. The EOS effects are more pronounced in the case of the rate of the frequency $d\nu/dt$ as indicated in Fig. 12(b). A stiffer EOS leads to a higher value of the spindown rate. Only when the frequency approaches the critical value, the spindown rate appears to be model independent.

In Fig. 12(c) I plot the dependence of the spindown rate $d\nu/dt$ on the frequency. For the same values of the frequency a higher value of L leads to a larger value of the spindown rate (the neutron star approaches its critical frequency faster). It is worthwhile to notice that the results presented in Fig. 12(c) are sensitive both to the core temperature and mainly to the values of the r-mode amplitude α . The most interesting feature of this plot is related with the range covered by the implied equation of states. Thus, in the same figure I include the observed spin-down rate for three cases (IGR J00291+5934, XTE J1751-305 and SAX J1808-3658) in comparison with the theoretical predictions [53, 54, 55, 56, 57, 58]. I estimate that it may be possible, by a suitable treatment of observations and related theoretical predictions of the spin frequency and spindown rate of known neutron star, to impose additional constraints on the nuclear equation of state. However, it is necessary to proceed with a more detailed calculation concerning the r-mode instability and evolution. In order to establish the above statement is necessary to use more elaborate equations of state (with additional degrees of freedom), to consider additional dissipation mechanisms and treat more carefully the thermal evolution.

It should be noted that in the present analysis additional degrees of freedom, like quark and hyperon matter are not considered for the construction of the equation of state. It is known that, in most cases, the presence of quark and hyperon matter affect appreciably the equation of state by softening the density dependence mainly for high densities. This means that the bulk properties of neutron stars will also be affected and consequently the time scales of the r-mode will be affected too. In addition, the presence of quark and hyperons influence the dissipation mechanisms since one has to take into account the shear and also the bulk viscosities due to the presence of this kind of matter. Actually, there are several recent studies in this direction [20, 21, 59, 60, 61, 62, 63, 64]. In any case, when more degrees of freedom are taken into account, the analysis becomes more complete and consequently more reliable.

In view of the above discussion, I consider that another issue worth examining is the connection between the observed neutron stars in low-mass X-ray binaries and the nuclear physics input via the equation of state [65, 66, 67]. It would be very interest, if it is possible to constrain the nuclear physics input (for example the slope parameter L) employing the related observation data. In general, this is a very complex problem, since the nuclear equation of state affects in different ways the r-mode instability and consequently additional work is needed as well as one has to illustrate further this point. However additional theoretical and observational work must be dedicated before being able to impose strong constraints on the implemented EOSs.

Finally, it is well known that for high temperature $T > 10^{10}$ K, which characterize mainly a newborn neutron star, the bulk viscosity is the dominant dissipation mechanism. However such a kind of dissipation is not considered in the present work. Actually, at high temperature, in a self-consistent treatment one has to consider also temperature effects on the nuclear equation of state. It is known [68] that temperature influences not only the density dependence of the equation of state but in addition both the transition density and the proton fraction. Actually the present MDIM model can be extended to include also the temperature effect on equation of state [30, 31, 32, 33, 34]. Work along these lines is in progress.

5 Summary

In the present work I consider the effect, on r-mode instability, due to the presence of a solid crust in a neutron star. By employing a phenomenological nuclear model I calculated the equation of state of β -stable matter which characterizes the neutron star core and is used for the location of the transition density at the inner edge between the liquid core and the solid crust. The stiffness of the equation of state parameterized via the slope parameter L , was varied on the interval $72.5 \text{ MeV} \leq L \leq 110 \text{ MeV}$. The gravitational and the viscous time scales depend directly on the parameter L as well as indirectly on the transition density n_t . As a consequence the critical angular velocity as well as the critical temperature depend on the equation of state. I found also that the instability window drops by $\simeq 20 - 40$ Hz when the mass of a neutron star is raised from $M = 1.4M_\odot$ to $M = 1.8M_\odot$ and also that the use of a stiffer equation of state increases the instability window. I compared the r-mode instability window for the five selected equation of states with those of the observed neutron stars in LMXBs and MSRPs for $M = 1.4M_\odot$ and $M = 1.8M_\odot$. I found that the majority of the stars lie outside of the instability windows. Finally, I estimated the time evolution of the spin frequency and spin-down rate for the selected EOS's for a $M = 1.4M_\odot$ neutron star mass in comparison with three observed cases. I conclude that it may be possible to impose additional constraints on the nuclear equation of state, by a suitable combination of observations and relative theoretical predictions.

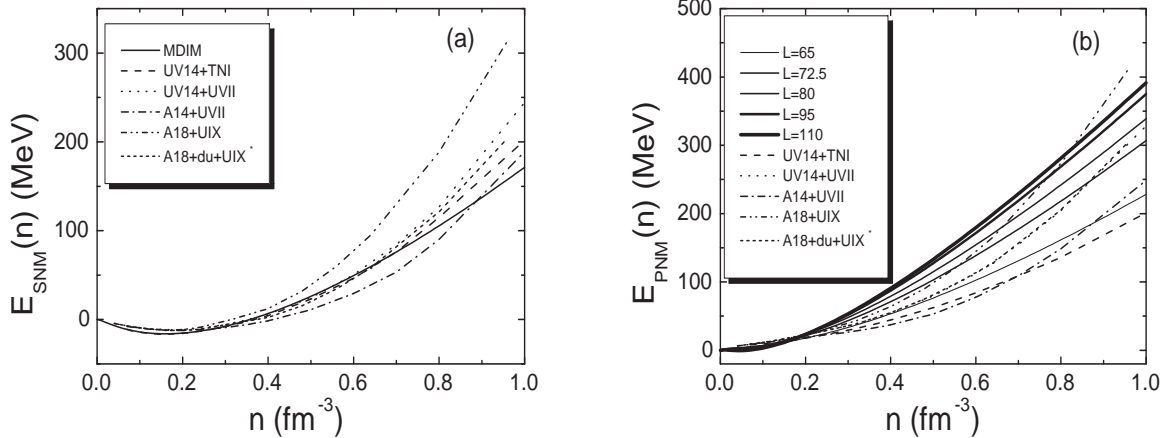


Figure 1: The energy per baryon of symmetric nuclear matter (a) and pure neutron matter (b), as a function of the baryon density n , of the present model (MDIM) in comparison with those originating from realistic calculations. More details for the models UV14+TNI, UV14+UVII and AV14+UVII in Ref. [35] and for the models A18+UIX and A18+du+UIX* in Ref. [36].

Acknowledgments

This work was supported by the German Science Council (DFG) via SFB/TR7 and by the Aristotle University of Thessaloniki Research Committee under Contract No. 89286. The author would like to thank the Theoretical Astrophysics Department of the University of Tuebingen, where part of this work was performed and Professor K. Kokkotas for his useful comments on the preparation of the manuscript. The author thanks Dr. C.P. Panos for his remarks on the present paper and Dr. A. Mytidis for useful discussions.

Table 1: The slope parameter L (in MeV), the transition density n_t (in fm^{-3}), the transition pressure P_t (in MeV fm^{-3}), the total radius R (in km), the core radius R_c (in km), the core mass M_c in M_\odot and the central pressure P_c (in MeV fm^{-3}) correspond to a neutron star with mass $M = 1.4M_\odot$.

| L | n_t | P_t | R | R_c | M_c | P_c |
|------|--------|--------|--------|--------|-------|-------|
| 65 | 0.0781 | 0.317 | 11.885 | 10.956 | 1.383 | 86.4 |
| 72.5 | 0.0730 | 0.319 | 12.725 | 11.631 | 1.379 | 63.2 |
| 80 | 0.0693 | 0.295 | 13.041 | 11.898 | 1.378 | 57.5 |
| 95 | 0.0587 | 0.155 | 13.490 | 12.385 | 1.386 | 49.2 |
| 110 | 0.0456 | 0.0188 | 13.646 | 12.805 | 1.397 | 43.5 |

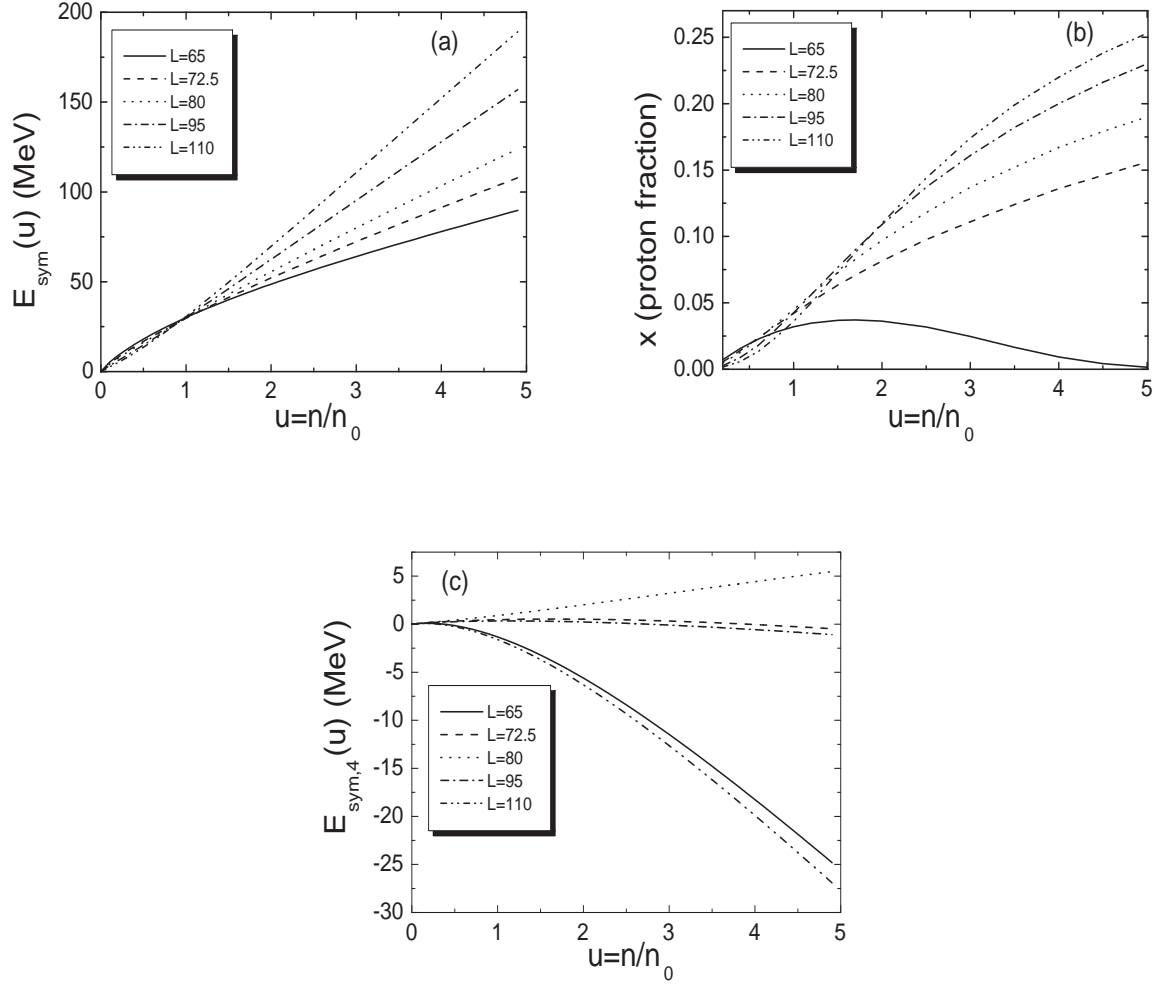


Figure 2: The nuclear symmetry energy (a) the proton fraction (b) and the fourth order term $E_{\text{sym},4}(u)$ of the symmetry energy (c) as a function of the ratio $u = n/n_0$ for various values of the slope parameter L .

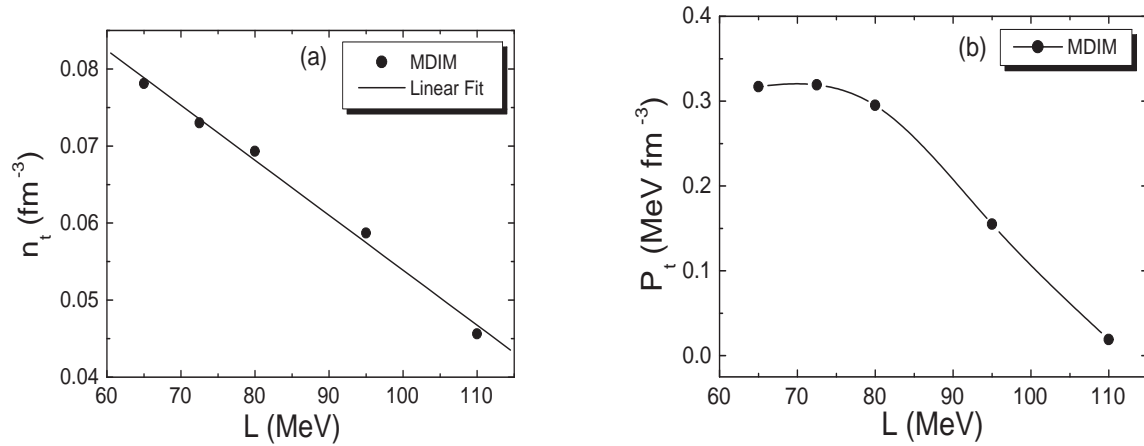


Figure 3: The transition baryon density n_t (a) and the transition pressure P_t (b) as a function of the slope parameter L . For more details about the linear fit see text.

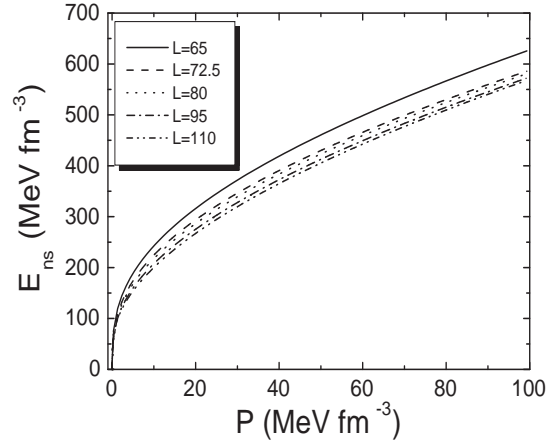


Figure 4: The energy density E_{ns} , taking into account both the fluid core and the solid crust matter, of neutron star matter as a function of the pressure P for various values of the slope parameter L . The data used for densities lower than the transition density n_t have been taken from [24] and [25] (for more details see text).

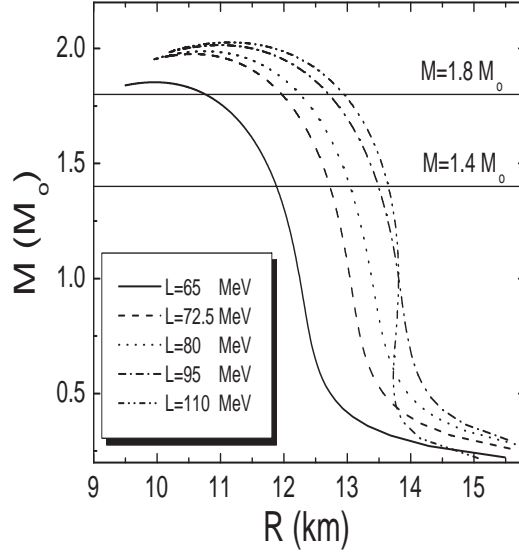


Figure 5: The mass-radius relations for the selected EOSs

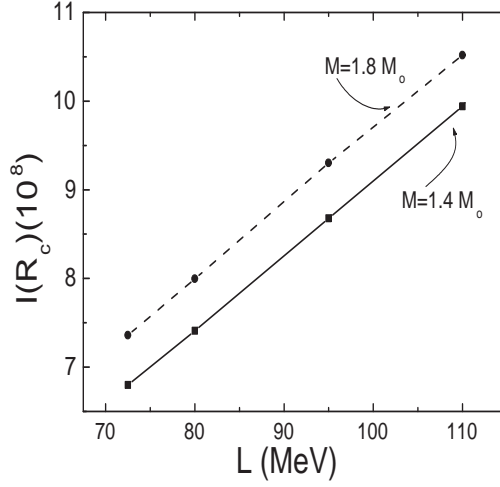


Figure 6: The values of the fundamental integral $I(R_c) = \int_0^{R_c} \epsilon(r)r^6 dr$ as a function of the slope parameter L for the interval $72.5 \text{ MeV} \leq L \leq 110 \text{ MeV}$. For more details about the linear fit see text.

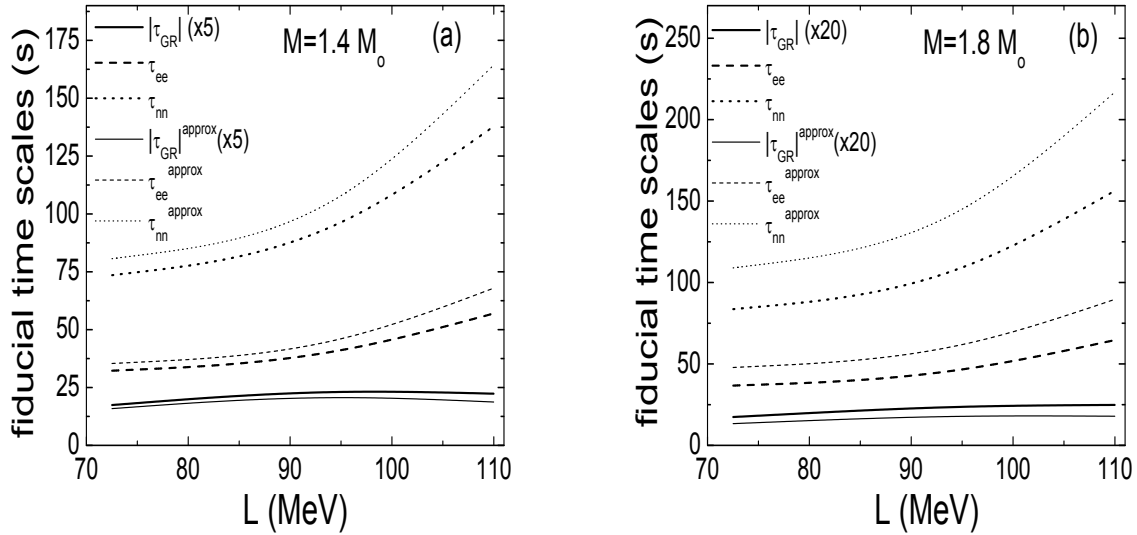


Figure 7: The fiducial time scales $\tilde{\tau}_{GR}$, $\tilde{\tau}_{ee}$, $\tilde{\tau}_{nn}$ as well as $\tilde{\tau}_{GR}^{approx}$, $\tilde{\tau}_{ee}^{approx}$, $\tilde{\tau}_{nn}^{approx}$ as a function of the slope parameter L for a neutron star with mass $M = 1.4M_\odot$ (a) and $M = 1.8M_\odot$ (b). In case $M = 1.4M_\odot$ the gravitational times scales are multiplied by a factor 5 and in case $M = 1.8M_\odot$ are multiplied by a factor 20.

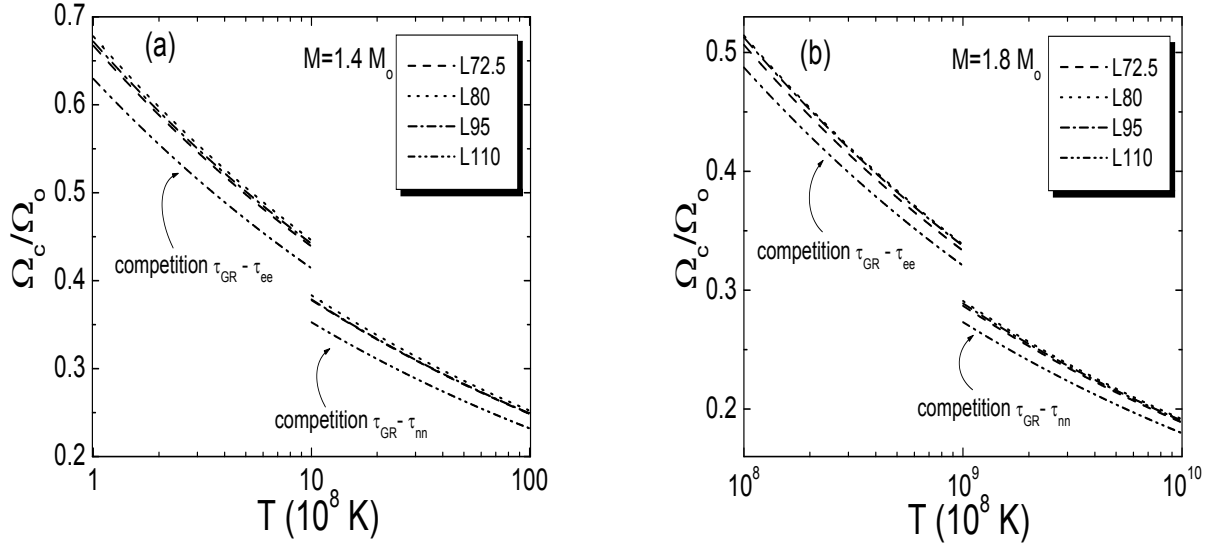


Figure 8: Temperature dependence of the critical angular velocity ratio Ω_c/Ω_0 for a neutron star with mass $M = 1.4M_\odot$ (a) and $M = 1.8M_\odot$ (b) constructed for the selected EOSs.

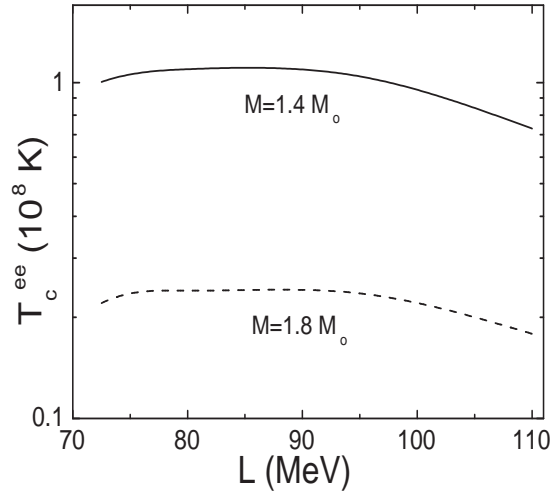


Figure 9: The critical temperature as a function of the slope parameter L for a neutron star with mass $M = 1.4M_\odot$ and $M = 1.8M_\odot$.

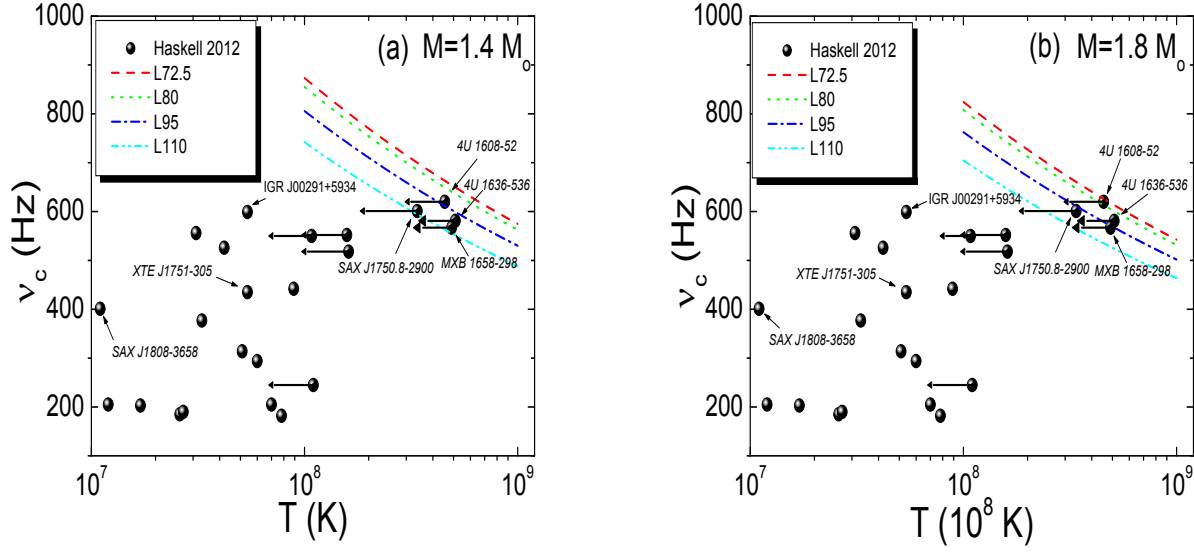


Figure 10: (Color online) The critical frequency temperature dependence for a neutron star with mass $M = 1.4M_{\odot}$ (a) and $M = 1.8M_{\odot}$ (b) constructed for the selected EOSs. The observed cases of LMXBs and MSRPs from Haskell et al. [21], are also included for a comparison. The horizontal vectors extending leftward exhibit the uncertainties of the core temperature. The cases *IGR J00291+5934*, *XTE J1751-305* and *SAX J1808-3658* with well known observation spindown rate, are also indicated (see also Fig.12(c)).

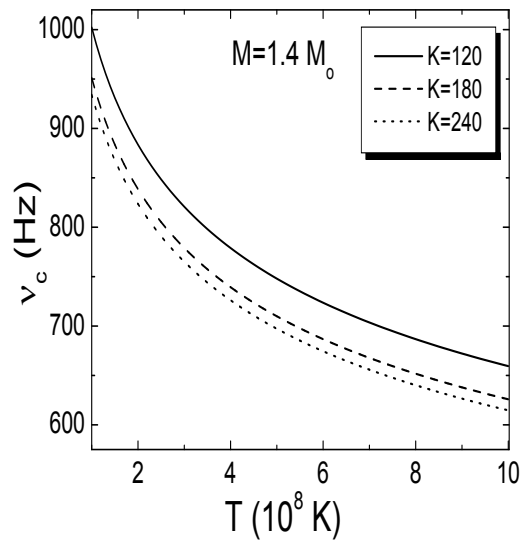


Figure 11: The critical frequency temperature dependence for a neutron star with mass $M = 1.4M_{\odot}$ for a fixed $E_{sym}(u)$, given by Eq. (62) and for three values of the incompressibility K .

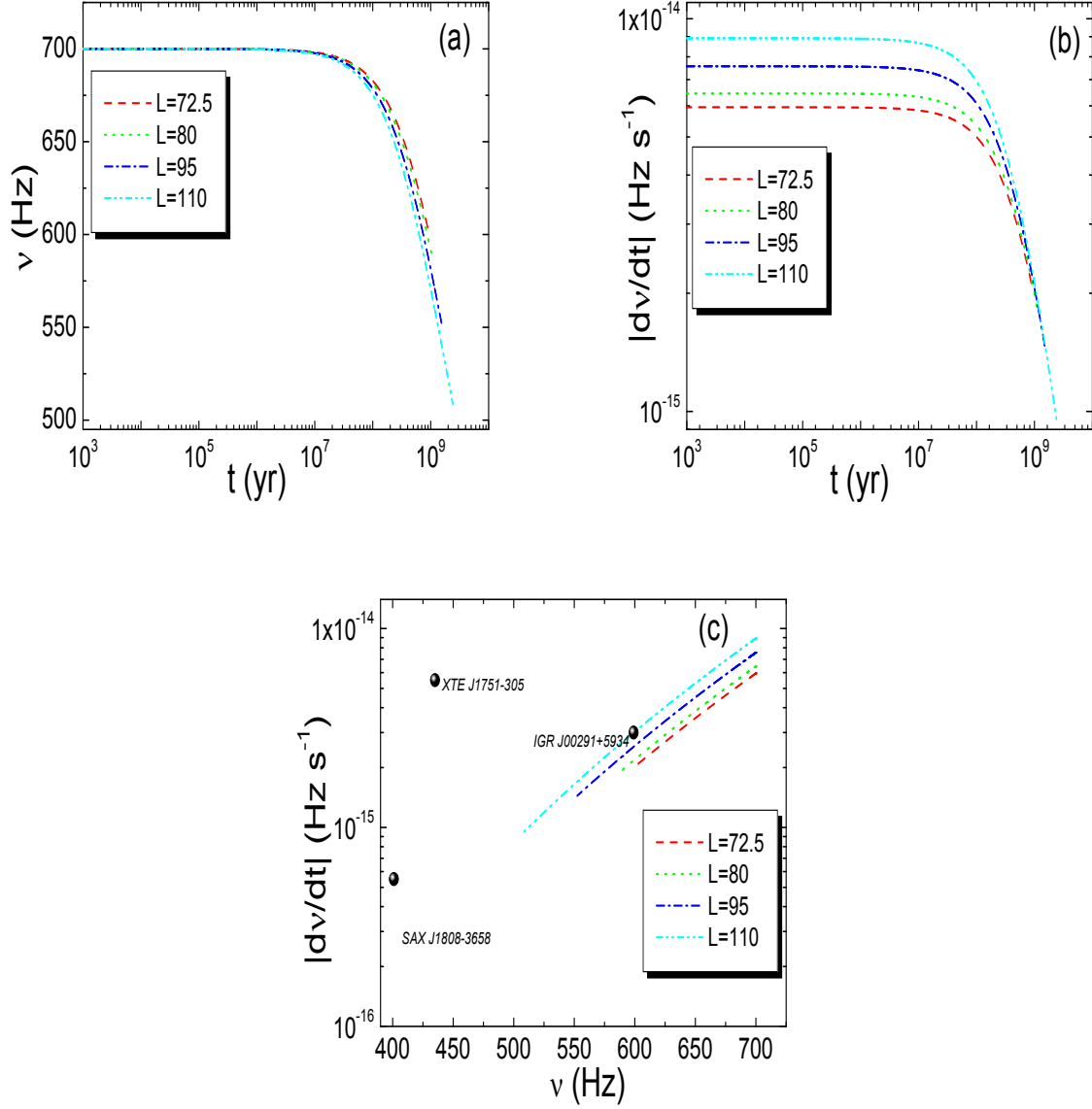


Figure 12: (Color online) (a) The time evolution of the spin frequency, (b) the spin-down rate evolution, for a neutron star with mass $M = 1.4M_{\odot}$, for the selected EOS and (c) the spin-down rate versus the spin frequency, for the selected EOS compared to three observed pulsars data [53, 55].

Table 2: The same as in Table 1 for $M = 1.8M_{\odot}$.

| L | n_t | P_t | R | R_c | M_c | P_c |
|------|--------|--------|--------|--------|-------|-------|
| 65 | 0.0781 | 0.317 | 10.757 | 10.287 | 1.793 | 331 |
| 72.5 | 0.0730 | 0.319 | 11.965 | 11.328 | 1.788 | 176 |
| 80 | 0.0693 | 0.295 | 12.253 | 11.584 | 1.788 | 159 |
| 95 | 0.0587 | 0.155 | 12.706 | 12.052 | 1.792 | 133.5 |
| 110 | 0.0456 | 0.0188 | 12.951 | 12.444 | 1.798 | 117 |

Table 3: The fiducial time scales (in sec) for a neutron star with mass $M = 1.4M_{\odot}$

| L | $\tilde{\tau}_{GR}$ | $\tilde{\tau}_{GR}^{approx}$ | $\tilde{\tau}_{vee}$ | $\tilde{\tau}_{vee}^{approx}$ | $\tilde{\tau}_{vnn}$ | $\tilde{\tau}_{vnn}^{approx}$ |
|------|---------------------|------------------------------|----------------------|-------------------------------|----------------------|-------------------------------|
| 72.5 | -3.484 | -3.176 | 32.254 | 35.380 | 73.526 | 80.656 |
| 80 | -3.986 | -3.637 | 33.833 | 37.076 | 77.637 | 85.076 |
| 95 | -4.615 | -4.123 | 41.125 | 46.035 | 96.377 | 107.882 |
| 110 | -4.468 | -3.748 | 56.977 | 67.936 | 137.840 | 164.353 |

References

- [1] L. Lindblom, B.J. Owen, and G. Ushomirsky, Phys. Rev. D **62**, 084030 (2000).
- [2] S.L. Shapiro and S.A. Teukolsky, *Black Holes, White Dwarfs, and Neutron Stars* (John Wiley and Sons, New York, 1983).
- [3] N.K. Glendenning, *Compact Stars: Nuclear Physics, Particle Physics, and General Relativity*, (Springer, Berlin, 2000)
- [4] P. Haensel, A.Y. Potekhin, and D.G. Yakovlev, *Neutron Stars 1: Equation of State and Structure* (Springer-Verlag, New York, 2007).
- [5] N. Andersson, Astroph. J. **502**, 708 (1998).
- [6] J.L. Friedman and S.M. Morsink, Astroph. J. **502**, 714 (1998).
- [7] J.L. Friedman and K.H. Lockitch, Prog. Theor. Phys. Suppl. **136**, 121 (1999).
- [8] N. Andersson and K.D. Kokkotas, Int. J. Mod. Phys. D **10**, 381 (2001).
- [9] N. Andersson, Class. Quantum Grav. **20**, R105 (2003).
- [10] K.D. Kokkotas and N. Stergioulas, Astron. Astrophys. **341**, 110 (1999).
- [11] N. Andersson, K. Kokkotas, and B.F. Schutz, Astroph. J. **510**, 846 (1999).
- [12] K.D. Kokkotas, *Gravity, Astrophysics, and Strings '02* (Eds. P.P. Fiziev and M.D. Todorov, St. Kliment Ohridski University Press, Sofia, 2003).
- [13] N. Andersson, *r-mode runaway in rapidly rotating neutron stars*, ICTP Lecture Notes Series, *Gravitational Waves: A Challenge to Theoretical Astrophysics*, Volume III, 297 (2001).
- [14] L. Lindblom, *Neutron star pulsations and instabilities*, ICTP Lecture Notes Series, *Gravitational Waves: A Challenge to Theoretical Astrophysics*, Volume III, 257 (2001).
- [15] L. Bildsten and G. Ushomirsky, Astroph. J. Lett. **529**, L33 (2000).
- [16] N. Andersson, D.I. Jones, K.D. Kokkotas, and N. Stergioulas, Astroph. J. **534**, L75 (2000).
- [17] M. Rieutord, Astroph. J. **550**, 443 (2001).
- [18] D.H. Wen, W.G. Newton, and B.A. Li, Phys. Rev. C **85**, 025801 (2012).

Table 4: The fiducial time scales (in sec) for a neutron star with mass $M = 1.8M_{\odot}$

| L | $\tilde{\tau}_{GR}$ | $\tilde{\tau}_{GR}^{approx}$ | $\tilde{\tau}_{vee}$ | $\tilde{\tau}_{vee}^{approx}$ | $\tilde{\tau}_{vnn}$ | $\tilde{\tau}_{vnn}^{approx}$ |
|------|---------------------|------------------------------|----------------------|-------------------------------|----------------------|-------------------------------|
| 72.5 | -0.870 | -0.668 | 36.686 | 47.792 | 83.629 | 108.946 |
| 80 | -0.992 | -0.760 | 38.415 | 50.145 | 88.150 | 115.068 |
| 95 | -1.182 | -0.890 | 46.613 | 61.889 | 109.238 | 145.036 |
| 110 | -1.241 | -0.895 | 64.628 | 89.664 | 156.349 | 216.920 |

- [19] I. Vidaña, Phys. Rev. C **85**, 045808 (2012); Erratum Phys. Rev. C **90**, 029901 (2014).
- [20] M.G. Alford, S. Mahmoodifar, and K. Schwenzer, Phys. Rev. D **85**, 024007 (2012).
- [21] B. Haskell, N. Degenaar, W.C.G. Ho, Mon. Not. R. Astron. Soc. **424**, 93 (2012).
- [22] S. Yoshida and U. Lee, Astrophys. J. **546**, 1121 (2001).
- [23] Y. Levin and G. Ushomirsky, Mon. Not. R. Astron. Soc. **324**, 917 (2001).
- [24] R.P. Feynman, N. Metropolis and E. Teller, Phys. Rev. **75**, 1561 (1949).
- [25] G. Baym, C. Pethik and P. Sutherland, Astrophys. J. **170**, 299 (1971).
- [26] B.J. Owen, L. Lindblom, C. Cutler, B.F. Schutz, A. Vecchio, and N. Andersson, Phys. Rev. D **58**, 084020 (1998).
- [27] L. Lindblom, B.J. Owen, and S.M. Morsink, Phys. Rev. Lett., **80**, 4843 (1998).
- [28] R. Bondarescu, S.A. Teukolsky, and I. Wasserman, Phys. Rev. D **79**, 104003 (2009).
- [29] Madappa Prakash, I. Bombaci, Manju Prakash, P.J. Ellis, J.M. Lattimer, R. Knorren, Phys. Rep. **280**, 1 (1997).
- [30] V.P. Psonis, Ch.C. Moustakidis, and S.E. Massen, Mod. Phys. Let. A **22**, 1233 (2007).
- [31] Ch.C. Moustakidis, Phys. Rev. C **76**, 025805 (2007).
- [32] Ch.C. Moustakidis, Phys. Rev. C **78**, 054323 (2008).
- [33] Ch.C. Moustakidis and C.P. Panos, Phys. Rev. C **79**, 045806 (2009).
- [34] Ch.C. Moustakidis, Int. J. Mod. Phys. D, **18**, 1205 (2009).
- [35] R.B. Wiringa, V. Fiks, and A. Fabrocini, Phys. Rev. C **38**, 1010 (1988).
- [36] A. Akmal, V.R. Pandharipande, and D.G. Ravenhall, Phys. Rev. C **58**, 1804 (1998).
- [37] M. Prakash, *The Equation of State and Neutron Stars* lectures delivered at the Winter School held in Puri India (1994).
- [38] J.M. Lattimer and M. Prakash, Phys. Rep. **442**, 109 (2007).
- [39] H.B. Callen, Thermodynamics, Wiley, New York, 1985.
- [40] Ch.C. Moustakidis, T. Nikšić, G.A. Lalazissis, D. Vretenar, and P. Ring, Phys. Rev. C **81**, 065803 (2010).
- [41] J. Xu, L.W. Chen, B.A. Li, and H.R. Ma, Astrophys. J. **697**, 1549 (2009).
- [42] C. Ducoin, J. Margueron, and C. Providência, Eur. Lett. **91**, 32001 (2010).
- [43] C. Ducoin, J. Margueron, C. Providência and I. Vidaña, Phys. Rev. C **83**, 045810 (2011).
- [44] B. Link, R.I. Epstein, and J.M. Lattimer, Phys. Rev. Lett., **83**, 3362, (1999).
- [45] J.M. Lattimer and M. Prakash, Astrophys. J. **550**, 426 (2001).
- [46] Ch.C. Moustakidis, Phys. Rev. C **86**, 015801 (2012).

- [47] A.L. Watts, B. Krishnam, L. Bildsten, and B.F. Schutz, *Mon. Not. R. Astron. Soc.* **389**, 839 (2008).
- [48] L. Keek, D.K. Galloway, J.J. M. in't Zand, and A. Heger, *Astrophys. J.* **718**, 292 (2010).
- [49] W.C.G. Ho, N. Andersson, and B. Haskell, *Phys. Rev. Lett.*, **107**, 101101 (2011).
- [50] K. Glampedakis and N. Andersson, *Phys. Rev. D* **74**, 044040 (2006).
- [51] Y. Levin, *Astrophys. J.* **517**, 328 (1999).
- [52] R. Bondarescu, S.A. Teukolsky, and I. Wasserman, *Phys. Rev. D* **76**, 064019 (2007).
- [53] S. Mahmoodifar and T. Strohmayer, *Astrophys. J.* **773**, 140 (2013).
- [54] M.G. Alford and K. Schwenzer, *Proceedings of Science, Xth Quark Confinement and the Hadron Spectrum*, **258** (2013). (arXiv: 1302.2649 [astr-ph]).
- [55] R.N. Manchester, G.B. Hobbs, A. Teoh, and M. Hobbs, *Astron. J.* **129**, 1993 (2005).
- [56] A. Patruno, *Astroph. J* **722**, 909 (2010).
- [57] A. Patruno, *et al.*, *Astroph. Journ. Lett.* **746**, L27 (2012).
- [58] A. Patruno and A. Watts, arXiv:1206.2727.
- [59] N. Andersson, B. Haskell, and G.L. Comer, *Phys. Rev. D* **82**, 023007 (2010).
- [60] B. Haskell, N. Andersson, D.I. Jones, and L. Samuelsson, *Phys. Rev. Lett.*, **99**, 231101 (2007).
- [61] M.G. Alford, S. Mahmoodifar, and K. Schwenzer, *Phys. Rev. D* **85**, 044051 (2012).
- [62] L. Lindblom and B.J. Owen, *Phys. Rev. D* **65**, 063006 (2002).
- [63] G. Rupak and P. Jaikumar, *Phys. Rev. C* **88**, 065801 (2013).
- [64] D. Chatterjee and D. Bandyopadhyay, *Astrophys. Space Sci.* **308**, 451 (2007).
- [65] J. S. Read, C. Markakis, M. Shibata, K. Uryu, J.D. E. Creighton, and John L. Friedman, *Phys. Rev. D* **79**, 0124033 (2009).
- [66] J. S. Read, B.D. Lackey, B.J. Owen, John L. Friedman, *Phys. Rev. D* **79**, 0124032 (2009).
- [67] K. Takami, L. Rezzolla, and L. Baiotti, *Phys. Rev. Lett.*, **113**, 091104 (2014).
- [68] J. Xu, L.W. Chen, C.M. Ko, and B.A. Li, *Phys. Rev. C* **81**, 055805 (2010).